

Hydrodesulphurization of Thiophenes over CoMoRe/ ZSM 5 γ -Al₂O₃ Catalyst

RAMI DOUKEH¹, MIHAELA BOMBOS², MARIOARA MOLDOVAN³, ION BOLOCAN^{1*}

¹Petroleum Gas University of Ploiesti, Bucuresti 39 Blvd., 100680, Ploiesti, Romania

²National Research Institute for Chemistry and Petrochemistry, ICECHIM, 202 Spl. Independentei 202, 060021, Bucharest, Romania

³Babes-Bolyai University, Cluj-Napoca, Institute for Research in Chemistry Raluca Ripan, 30 Fantanele Str., Cluj Napoca, Romania

The hydrodesulphurization (HDS) of thiophenes was performed on metallic catalyst CoMoRe/ZSM5- γ -Al₂O₃. Experiments were carried out on a fixed bed catalytic reactor at 175-300°C, 30-60 atm, thiophene volume hourly space velocities of 1h⁻¹- 4h⁻¹ and molar ratio hydrogen/thiophene of 60/1. Texture features like specific surface area, the pore volume and the average pore diameter decrease after catalyst sulfuration. The thiophenes conversion on CoMoRe/ γ -Al₂O₃-Zn-HZSM 5 catalyst differs with the nature of the studied thiophenes.

Keywords: thiophenes, hydrodesulphurization, catalyst acidity

Hydrodesulfurization is the most important hydro-treatment process since the removal of sulfur from petroleum fractions is a priority for environmental protection [1, 2].

The distribution of sulfur compounds depends mainly on the origin of the crude oil. The type of compounds present, their reactivity, the reaction mechanism, the hydrodesulphurization kinetics, and the factors that influence the reactivity of the compounds with sulfur must be known to carry out the desulfurization process. The sulfur compounds most studied are thiols, sulfides, disulfides, thiophene, benzothiophene and dibenzo-thiophene [1,2]. The reactivity of sulfur compounds has long been studied and is significantly different. There are numerous possibilities for formulating hydrodesulfurization catalysts and their choice in refineries usually adapts to the characteristics of petroleum fractions and refined product specifications.

The most used catalysts have the active component in the form of molybdenum or tungsten sulfide, to which cobalt and nickel are added as promoters. Other possibilities are Ni-Mo, Ni-W, or Co-W less often [3]. Catalysts are prepared in such a way to give a larger surface and a proper pore structure and sometimes are added in small amounts of promoters in order to increase the activity of the metal sulfide [4].

One of the research directions in this field relates to the use of new types of catalytic supports. Mesoporous silica is an alternative to the use of alumina due to the ordered hexagonal structure of mesopores and the large specific surface having a catalytic potential for reactions involving bulky molecules, including hydrodesulphurization of petroleum fractions [5, 6]. have been very studied for this type of reaction [7, 8]. The use of SBA-15 support for hydrotreating catalysts has some advantages over mesoporous solids HMS or MCM 41, such as lower pore wall thicknesses and higher hydrothermal stability, properties important for hydrotreatment processes due to the severe conditions involved [9].

Zeolite ZSM 5, is a synthetic zeolite with secondary unit construction unit T₁₂O₂₄ (tetrahedral-octahedron unit) containing 5-membered rings [10]. These units form chains, which interconnect leads to the formation of the space network. Zeolite ZSM-5 crystallizes easily in a wide range of composition corresponding to the molar SiO₂/Al₂O₃

molar ratio of 20. The higher the SiO₂/Al₂O₃ molar ratio, the more crystallization occurs. There are numerous synthetic methods and a wide range of organic additives have been tested to form the zeolite ZSM 5 structure [11].

In this paper, a hydrodesulfurization catalyst with improved acidity by the addition of Re pentoxide and a zinc-modified ZSM5 zeolite during the crystallization process was studied.

Experimental part

Catalysts synthesis

The materials used for catalyst syntheses were cobalt (II) nitrate hexahydrate puriss p.a. (Sigma-Aldrich), ammonium heptamolybdate tetrahydrate (Sigma-Aldrich), perhenic acid solution (Sigma-Aldrich), Zn-HZSM5 and γ -alumina granulated with the average size of 1 mm. Appropriate amounts of an aqueous solution of ammonium heptamolybdate tetrahydrate, cobalt (II) nitrate hexahydrate, and perhenic acid were used as starting materials. Mo precursor was first impregnated followed by Re and Co. The method of pore filling by successive steps was employed for depositing of the three metals. The concentration of precursors was calculated according to the desired metal content. The metal loadings was at about 8% Mo, 4% Co and 0.5% Re. After each impregnation step, the material was dried at ambient temperature for 24 hours and calcined at 450°C for 6 h.

Catalyst characterization

Textural characteristics of the catalyst were determined by BET analysis on Autosorb1 Quantacrome instrument. Thus the specific surface area (S_{BET}) was determined by BET method in the linear portion of the adsorption-desorption isotherm.

The acid strength distribution has been determined by the thermal desorption of diethylamine on a DuPont Instruments Thermal Analyst 2000/2100 coupled with a module 951 Thermogravimetric Analyzer and the morphological analysis of the catalysts by electronic scanning microscopy (SEM) was performed using a FEI Inspect microscope, model S, with a voltage range of 200V-30kV.

FTIR spectra of the catalysts were obtained on a FTIR Jasco 610 spectrometer with the ATR method, in the range

* email: ibolocan@upg-ploiesti.ro

of 4000 to 550 cm^{-1} , at a scanning rate of 4 $\text{cm}^{-1} \cdot \text{s}^{-1}$, with an average of 128 measurements for each spectrum and characterization of X-ray diffraction catalysts was performed with the aid of a BRUKER D8 Advance X-ray apparatus using $\text{CuK}\alpha$ ($\lambda = 0.154 \text{ nm}$) radiation.

Hydrodesulphurisation tests

The catalyst was activated in a fixed bed reactor using hydrogen stream (electrolytic hydrogen purity from Linde Company) with a flow rate of 15 L/h at 450°C for 6 h. The activity of Co-Mo-Re/ $\gamma\text{-Al}_2\text{O}_3$ -Zn-HZSM5 catalyst was determined in the same reactor used in other studies [12,13] under isothermal conditions. An amount of 40 cm^3 catalyst was loaded in the middle of the reactor and the top and the bottom of the reactor were filled with inert glass beads with the average diameter of 1-2 mm. The temperature along the reactor was adjusted using an automatic system with two thermocouples placed in the reactor shell. The value of the temperature along the reactor was checked with the help of a movable thermocouple placed in the reactor jacket. The composition of the liquid phase is shown in table 1.

Table 1
THE COMPOSITION OF THE LIQUID PHASE

No. crt.	Component	Concentration, %wt.
1	Thiophene	0.125
2	Ethylthiophene	0.175
3	Benzothiophene	0.2
4	Hexane	99.5

The liquid phase reactor feeding was performed with the aid of a metering pump. The effluent was cooled at the exit of the reactor in a heat exchanger and the liquid phase was separated from the gaseous phase in a vertical gas-liquid separator. Hydrogen to thiophenes molar ratio of 60 was maintained constant in all tests. Reaction conditions were:

- temperature: 200-275°C;
- pressure: 30-60 atm;
- volume hourly space velocities of thiophenes (LHSV): 2-8 h^{-1} ;
- molar ratio hydrogen/ thiophenes: 60/1.

The reaction product were collected under stationary regime conditions and analyzed by gas chromatography (Varian 3800) coupled with mass spectrometry (Varian 4000). The GC was equipped with Agilent VF-5ms capillary column. The carrier gas was He, the oven temperature 175°C (16°C/min) and the injector temperature was 155°C.

Results and discussions

Catalyst characterization

The isotherm of adsorption / desorption and the pore-size distribution curves for catalyst Co-Mo-Re / $\gamma\text{-Al}_2\text{O}_3$ -Zn-HZSM5 is shown in figure 1. The isotherm is specific for capillary condensation process on mesoporous solid materials with low affinity for molecules adsorbed and a narrow distribution of pore sizes.

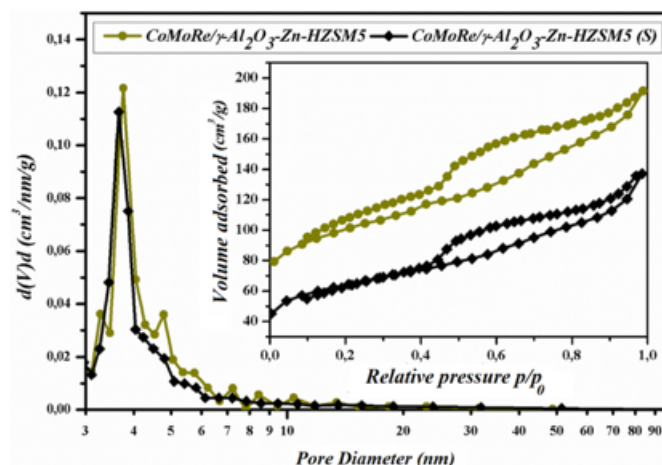


Fig. 1. The adsorption /desorption isotherm and the pore-size distribution curves for Co-Mo-Re / $\gamma\text{-Al}_2\text{O}_3$ -Zn-HZSM5 before sulphurization and after sulphurization, Co-Mo-Re / $\gamma\text{-Al}_2\text{O}_3$ -Zn-HZSM5 (S)

In the area of low relative pressure p/p_0 , the nitrogen volume adsorbed by the catalyst is associated with a monolayer adsorption of nitrogen on the surface. At relative pressure close to 1.0 it can be noted an increase in the volume adsorbed. The hysteresis loop, specific for multilayer condensation of nitrogen in the catalyst pores, is present on a wide range of vapor pressure. The isotherm alloy does not change, but a significant decrease in the porosity characteristics is observed after the sulfurization of the catalyst. This aspect was also reflected in the decrease of the specific surface after sulphurization from 122.15 m^2/g to 107.27 m^2/g .

The textural properties (BET surface area, pore volume and average pore diameter) of the sample are summarized in table 2. It can be noted a large surface area, pore volume relatively large and in single-mode mesopore size distribution, indicating good accessibility of the catalytic center. Texture features change after sulfurization; thus the specific surface area, the pore volume and the average pore diameter decreases, a decrease generated by the larger volume of the sulfur atoms compared to the oxygen that it has replaced.

The distribution of the acid center strength was determined by the thermal desorption of diethylamine. Figure 2 shows the thermal desorption curve of diethylamine for Co-Mo-Re / $\gamma\text{-Al}_2\text{O}_3$ -Zn-HZSM5 catalysts, before sulphurization and after sulphurization, and table 3 presents the data on the acid strength distribution for the two forms of the catalyst. Before sulphurization, it is observed a low content of medium and strongly acid centers (0.122 and 0.161 meq./g) and a concentration of approx. three times higher for the weak acidic centers (0.448 meq./g). After sulphurization, the concentration of medium and strongly acid centers increases, justified by the higher acidity of the sulphurized compounds than the oxygenated ones. Weak central concentration decreases obviously probably due to reduced accessibility of diethylamine to pores with lower acidity after sulphurization.

Specific Surface Area, m^2/g		Total pore volume, cm^3/g		Average pore diameter, nm	
Not sulphurized	Sulphurized	Not sulphurized	Sulphurized	Not sulphurized	Sulphurized
122.15	107.27	0.167	0.150	3.86	3.66

Table 2
TEXTURAL
CHARACTERISTICS OF
Co-Mo-Re / $\gamma\text{-Al}_2\text{O}_3$ -Zn-HZSM5 CATALYST, BEFORE
SULPHURIZATION AND
AFTER SULPHURIZATION

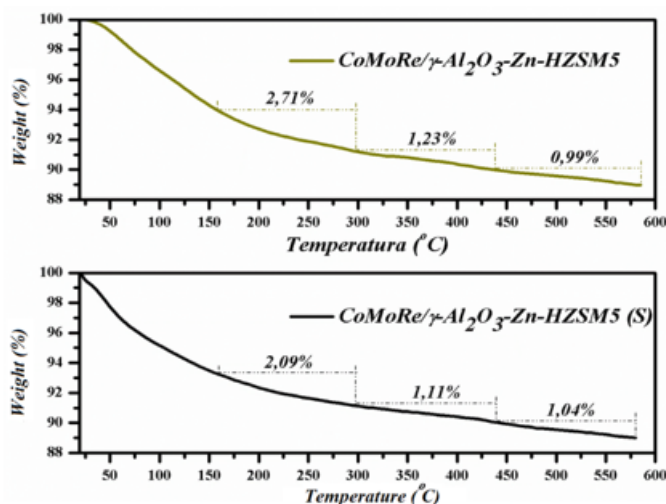


Fig.2. Thermal desorption curve of diethylamine for Co-Mo-Re / γ -Al₂O₃-Zn-HZSM5 catalyst before sulphurization and after sulphurization (Co-Mo-Re / γ -Al₂O₃-Zn-HZSM5 (S))

The IR spectra for the catalyst Co-Mo-Re / γ -Al₂O₃-Zn-HZSM5 (fig. 3) show several spectral bands due to Zn-modified HZSM5 zeolite. The main absorption bands, which are observed at approx. 1220 cm⁻¹ and 1100 cm⁻¹, correspond to SiO₄ asymmetrical stretching vibration and asymmetrical stretching vibration of the T-O-T structure (tetrahedral-octahedral tetrahedra), while at approx. 800, 560, and 460 cm⁻¹ correspond to the T-O-T deformation tensile vibration, respectively [14]. ZnO can not be identified because it has spectral bands at about 460 cm⁻¹ and 545 cm⁻¹ [15] overlapping with Mo-O specific bands which also have 560 cm⁻¹ or Si-O-Si spectral bands 466 cm⁻¹. After the sulfurization, the absorption maxima do not change but only the transmittance, which highlights the correctness of the spectrum interpretation.

Figure 4a and b show the SEM images of the CoMoRe catalyst. From the SEM analyzes it is observed that this

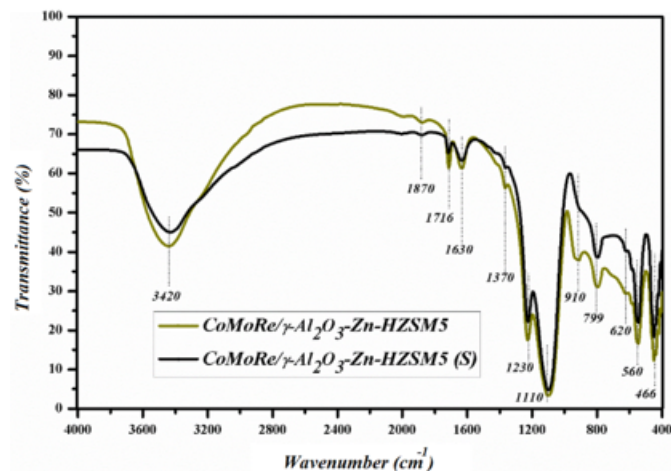


Fig.3. IR Spectra for Co-Mo-Re / γ -Al₂O₃-Zn-HZSM5 catalyst before and after sulfurization

Table 3

THE DISTRIBUTION OF ACIDITY STRENGTH FOR THE CATALYST
Co-Mo-Re / γ -Al₂O₃-Zn-HZSM5

Weak acidic centers		Medium-strength acid centers		Strong acidic centers		Total acidity	
Not sulphurized	Sulphurized	Not sulphurized	Sulphurized	Not sulphurized	Sulphurized	Not sulphurized	Sulphurized
0.448	0.319	0.122	0.149	0.161	0.217	0.731	0.685

catalyst is homogeneous in terms of the particle size distribution (fig. 40a).

Figure 5 shows the X-ray diffractogram of the catalyst before and after the sulfurization. It can be seen that the

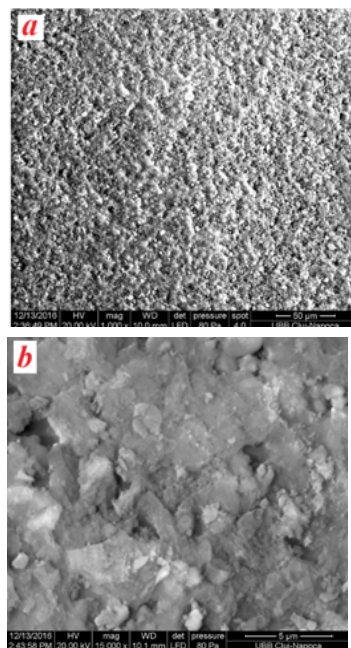


Fig.4. SEM images for the catalyst Co-Mo-Re / γ -Al₂O₃-Zn-HZSM5

catalyst prior to sulfurization exhibit intense XRD peaks which are specific for γ -Al₂O₃ support. The diffractogram show characteristic peaks at $2\theta \sim 36.7^\circ$; 45.5° and 66.8° [16]. The catalyst have undergone structural changes after sulfurization, either by decreasing the peak intensity or by dropping the specific peaks, indicating that the present species has been amorphous, or crystallites are too small to record a RX signal. After the sulfurization, Zn-HZSM 5 specific peaks are very well documented due to the amorphous transition of the sulfurized precursors whose signals do not overlap with those of the support. According to figure 5, this catalyst exhibits XRD peaks at $2\theta \sim 7.8^\circ$, 8.8° , 15.3° , 22.95° , 24° and 29.8° , which are according to HZSM 5 data.

Effect of temperature

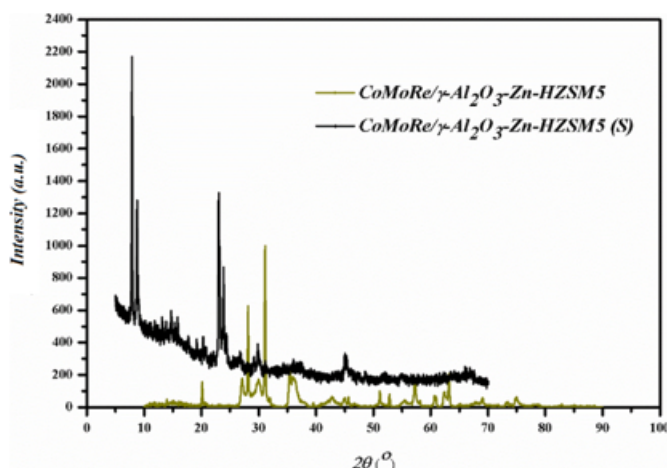


Fig.5. X-ray spectra of catalyst Co-Mo-Re / γ -Al₂O₃-Zn-HZSM5 before and after sulfurization

Studies of thiophenes conversion as a function of temperature are presented in figure 6 and the results shows that the activity of catalyst increased with the temperature. The higher conversions were achieved at 275°C. The conversion growth of thiophene was higher than that of ethylthiophene and benzothiophene across the range of temperature studied and the conversion growth of benzothiophene had the lowest values.

The products resulting from the hydrodesulfurization process identified in the effluent were ethyl-benzene, ethyl-

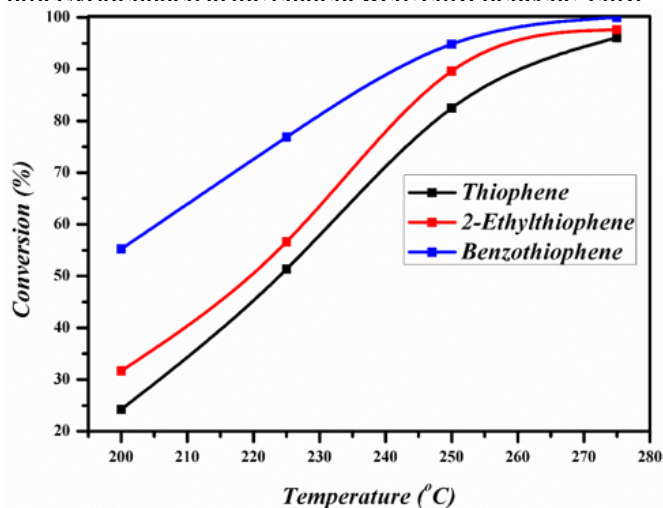


Fig. 6. The effect of temperature on thiophens conversion at 30 bar and LHSV 2 h⁻¹

tetrahydrothiophene and dihydro-benzothiophene. The influence of the temperature on the yield in these products at 30 bar and LHSV 2 h⁻¹, is shown in the figure 7. The yield in ethylbenzene increases with the temperature after a high slope curve, reaching a value of 100% at 275°C, while the yield in ethyl-tetrahydrothiophene is maintained at values close to 0% over the entire temperature range studied and the yield in dihydro-benzothiophene is lower than the yield in ethyl benzene and decreases to values close to 0% at a temperature of 275°C.

Effect of pressure

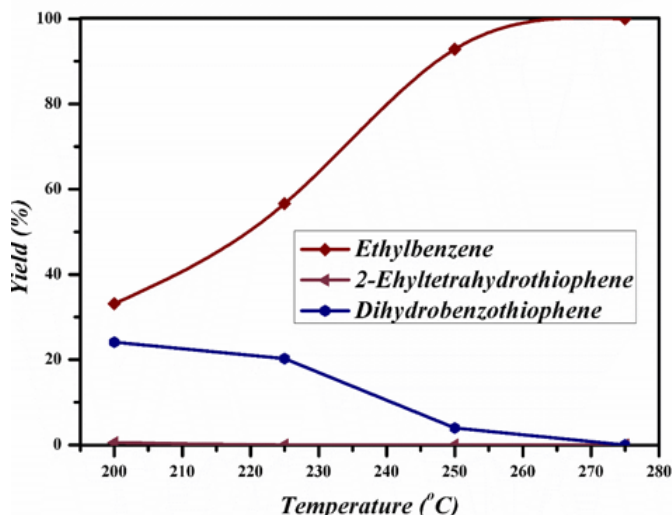


Fig. 7. The effect of temperature on yield in hydrodesulfurization products at 30 bar and LHSV 2 h⁻¹

From the figure 8 it is observed that the pressure had a significantly influence on the reactivity of ethylthiophene at 200°C and LHSV 2 h⁻¹. Also the conversion of thiophene and benzothiophene increased with the pressure but with a smaller slope of the variation curve. The conversion of

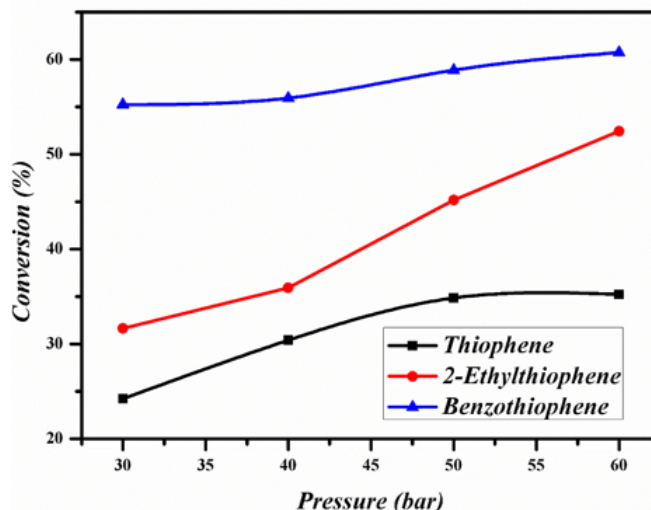


Fig. 8. The effect of pressure on thiophenes conversion at 200°C and LHSV 2 h⁻¹

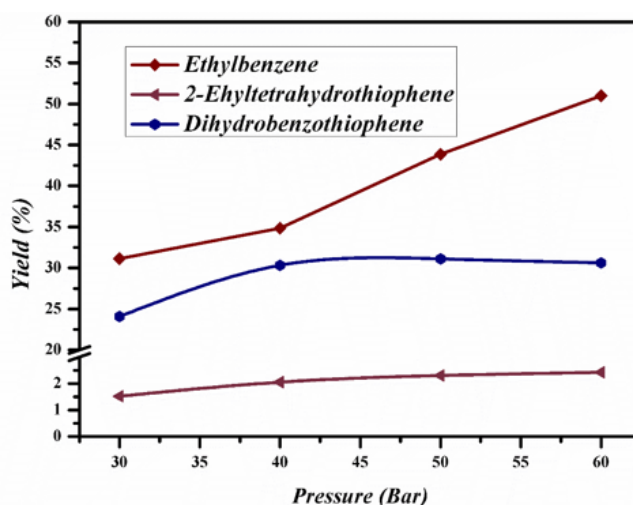


Fig. 9. The effect of pressure on yield in hydrodesulfurization products at 200°C and 30 bar

benzothiophene is much higher than the other two reactants across the range of pressures studied.

The influence of the pressure on the yield in ethylbenzene, ethyl-tetrahydrothiophene and dihydro-benzothiophene at 200 °C and LHSV 2 h⁻¹, is shown in the figure 9. The yield in ethylbenzene increases throughout the pressure range studied after a curve with a slope of nearly constant, while the yield in dihydro-benzothiophene is lower than that in ethylbenzene and varies very little with the pressure. The yield in ethyl-tetrahydrothiophene is much lower in the other two reaction products across the range of pressures studied.

Effect of volume hourly space velocities

Figure 10 showed the influence of volume hourly space velocities on thiophenes conversion at 30 bar and 275 °C. It can be seen that the conversion of the three reactants decreases with the increase of LH after curves with similar slopes.

Yield in ethylbenzene is much higher than in ethyl-tetrahydrothiophene and dihydro-benzothiophene and decreases with a slope of variation curves that increases with volume hourly space velocities (fig. 11). The yield in ethyl-tetrahydrothiophene and dihydro-benzothiophene increases with a different slope of the variation curves. Thus, the yield in dihydro-benzothiophene increases with a much higher yield than the yield in ethyl-tetrahydrothiophene

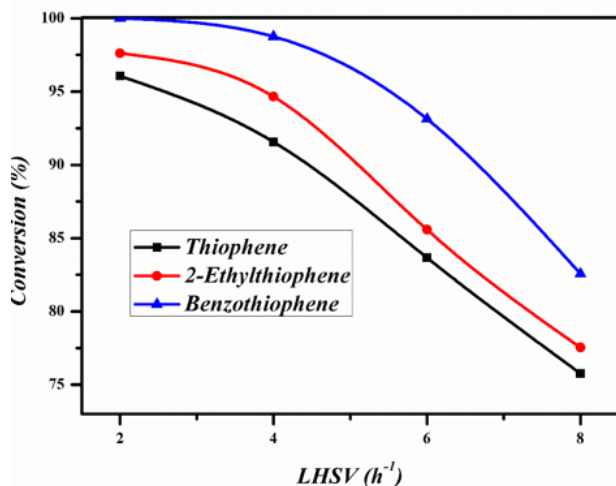


Fig. 10. Effect of LHSV on thiophenes conversion at 30 bar and 275°C

Conclusions

In the present work, CoMoRe/ γ -Al₂O₃-Zn-HZSM 5 catalyst was prepared by successive impregnation and characterized before and after sulfurization.

Texture features like specific surface area, the pore volume and the average pore diameter decrease after catalyst sulfurization, due to the larger volume of the sulfur atoms compared to the oxygen that it has replaced.

Also after sulphurization, the concentration of medium and strongly acid centers increases, justified by the higher acidity of the sulphurized compounds than the oxygenated ones. Weak central concentration decreases obviously probably due to reduced accessibility of diethylamine to pores with lower acidity after sulphurization.

The IR spectra for the catalyst Co-Mo-Re / γ -Al₂O₃-Zn-HZSM5 show several spectral bands due to Zn-modified HZSM5 zeolite. The main absorption bands, which are observed at approx. 1220 cm⁻¹ and 1100 cm⁻¹, correspond to SiO₄ asymmetrical stretching vibration and asymmetrical stretching vibration of the T-O-T structure (tetrahedral-octahedral tetrahedra), while at approx. 800, 560, and 460 cm⁻¹ correspond to the T-O-T deformation tensile vibration, respectively.

The SEM analyzes highlights that this catalyst is homogeneous in terms of the particle size distribution and the X-ray diffractogram of catalyst demonstrates structural changes after sulfurization, either by decreasing the peak intensity or by dropping the specific peaks, indicating that the present species has been amorphous, or crystallites are too small to record a RX signal.

The products resulting from the hydrodesulfurization process identified in the effluent were ethyl-benzene, ethyl-tetrahydrothiophene and dihydro-benzothiophene. The influence of pressure, temperature and volume hourly space velocities on the performance of the HDS process is similar to other tested catalysts.

References

- SERGE, R., *Conversia hidrocarburilor*. vol. 3. București, Editura Zecasin, 1997;
- SPEIGHT, J.G., *The chemistry and technology of petroleum*, 2014, CRC Press Taylor & Francis Group;
- DELGADO S., R.A., *Organometallic modeling of the hydrodesulfurization and hydrodenitrogenation reactions*, 2002, New York, Kluwer Academic Publishers;
- JONES D.S.J., *Handbook of petroleum processing*, 2006, Springer;

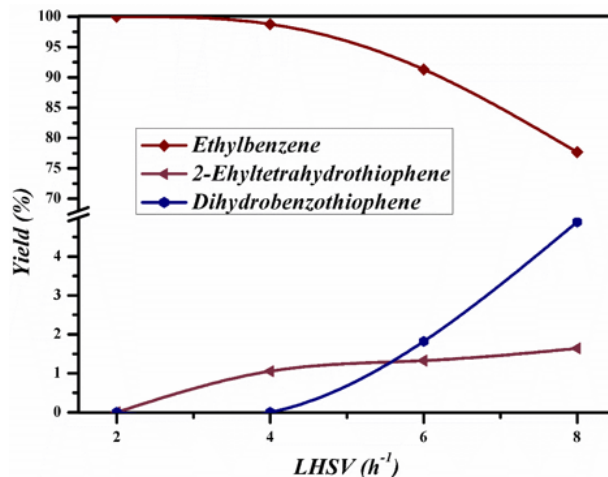


Fig. 11. Effect of LHSV on yield in hydrodesulfurization products at 30 bar and 275°C

- CORMA, A., MARTINEZ, A., MARTINEZSORIA, V., MONTON, J.B., Hydrocracking of Vacuum Gasoil on the Novel Mesoporous MCM-41 Aluminosilicate Catalyst, *Journal of Catalysis*, **153**, no.1, 1995. p. 25;
- SONG, C., MADHUSUDAN, R. K., Mesoporous molecular sieve MCM-41 supported Co-Mo catalyst for hydrodesulfurization of dibenzothiophene in distillate fuels. *Applied Catalysis A: General*, **176**, no.1, 1999, p. 1;
- NAVA, R., CASTANO, P., INFANTES-MOLINA, A., PAWELEC, B., Inhibition of CoMo/HMS catalyst deactivation in the HDS of 4,6-DMDBT by support modification with phosphate. *Fuel*, **90**, no.8, 2011, p. 2726;
- ZEPEDA, T.A., FIERRO, J. L. G., PAWELEC, B., NAVA, R., KLIMOVA, T., FUENTES, G. A., HALACHEV, T., Synthesis and Characterization of Ti-HMS and CoMo/Ti-HMS Oxide Materials with Varying Ti Content, *Chemistry of Materials*, **17**, no.16, 2005. p. 4062;
- VRADMAN, L., HERSKOWITZ, M., LANDAU, M.V., GEDANKEN, A., High loading of short WS₂ slabs inside SBA-15: promotion with nickel and performance in hydrodesulfurization and hydrogenation, *Journal of Catalysis*, **213**, no.2, 2003, p. 163;
- CEJKA, J., *Zeolites and Ordered Mesoporous Materials: Progress and Prospects*, vol. 157, Elsevier Science, 2005;
- SZOSTAK, R., *Handbook of molecular sieves*, New York, Van Nostrand Reinhold, 1952;
- DOUKEH, R., BOMBOS, M., TRIFOI, A., PASARE, M., BANU, I., BOLOCAN, I., Dimethyldisulphide Hydrodesulphurization on NiCoMo/Al₂O₃ Catalyst, *Rev.Chim. (Bucharest)*, **68**, no.7, 2017, p.1496
- DOUKEH, R., BOMBOS, M., TRIFOI, A., MIHAL, O., POPOVICI, D., BOLOCAN, BOMBOS, D., Kinetics of thiophene hydrodesulfurization over a supported Mo-Co-Ni catalyst, *Comptes Rendus Chimie*, **21**, 2018, p. 277;
- SU, X., BAI, X., WANG, G., ZHANG, J., Synthesis of nanosized HZSM-5 zeolites isomorphously substituted by gallium and their catalytic performance in the aromatization. *Chemical Engineering Journal*, **293**, 2016, p. 365;
- HANDORE, K., HORNE, A., BHAVSAR, S., CHABUKSWAR, V., Novel Green Route of Synthesis of ZnO Nanoparticles by Using Natural Biodegradable Polymer and Its Application as a Catalyst for Oxidation of Aldehydes, *Journal of Macromolecular Science, Part A*, **51**, no.12, 2014, p. 941;
- ZHANG, M.H., FAN, J., CHI, K., DUAN, A., ZHAO, Z., MENG, X., ZHAN, H., Synthesis, characterization, and catalytic performance of NiMo catalysts supported on different crystal alumina materials in the hydrodesulfurization of diesel, *Fuel Processing Technology*, **156**, 2017, p. 446

Manuscript received: 29.11.2017